ISBN: 978-3-95450-190-8 doi:10.18429/JACoW-ERL2017-MOPSPP008

LOW-ENERGY BEAM TRANSPORT SYSTEM FOR MESA*

C. Matejcek, K. Aulenbacher, S. Friederich, L. Hein, Institut für Kernphysik, Mainz, Germany

Abstract

An important part of the new accelerator MESA (Mainz energy-recovering superconducting accelerator) is the low-energy beam transport system connecting the 100 keV electron source with the injector accelerator. Here the spin manipulation and the bunch preparation for the injector accelerator take place. Due to the low energy, space charge will be an challenging issue in this part. Therefore, start-to-end simulations were done with a combination of the two particle dynamics codes PARMELA [1] and CST [2]. At the moment, a test setup is being built up to check the functionality of devices and compare the beam parameters with the simulation. Here the focus lies on the bunch preparation system because at this part we expect high impact of the space charge by reason of the necessary bunch compression. The advance of the test setup, the simulations and measurements done so far will be shown.

INTRODUCTION

A layout of the lattice of MELBA (MESA low-energy beam apparatus) can be seen in Figure 1. The electrons will be focused by quadrupoles and solenoids. Two times the beam will be bended by 270° by two alpha magnets. Several steerer magnets will correct the orbit of the electrons if it deviates from the reference orbit. Misalignment of the devices and magnetic stray fields will lead to such a deviation. One important part of MELBA is the spin manipulation consisting of two Wien filters and one solenoid. After the electrons are produced in the source, their spin is oriented in the longitudinal direction. The first Wien filter and the

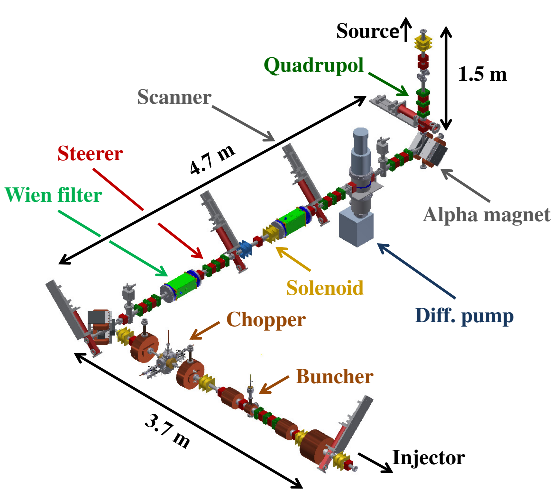

Figure 1: Layout of the low energy beam transport system for MESA.

* Work supported by the DFG within the GRK 2128; Cluster of exellence PRISMA

solenoid will align the spin in the horizontal direction. Compensation of further precession in the accelerator will be done by the second Wien filter. In principle the spin can be aligned in any direction with this arrangement. The reason for manipulation of the spin in this section is that the rotation angle of the Wien filter $\phi_{\text{spin, Wien}} \propto \frac{1}{\beta\gamma^2}$ and that of the solenoid $\phi_{\text{spin, sole}} \propto \frac{1}{\beta\gamma}$ [3]. So the required fields for spin rotation are small in this section. A challenging issue in this low-energy region is the transport of moderate bunch charges ($\mathcal{O}(1\,\text{pC})$) demanded by the experiment MAGIX (MESA gas internal target experiment). This is due to the fact that the space charge forces scale with $\frac{1}{\gamma^3}$. For offline characterisation of the beam, there are scanners installed, whereas for the online characterisation, there will be a xy monitor and a phase monitor. The second big part is the chopper and the buncher system responsible for matching the beam with the longitudinal acceptance of the injector where the beam will accelerated to an energy of 5 MeV. The chopper system consists of two circular deflecting cavities with a resonance frequency of 1.3 GHz, a solenoid ,and a collimator. For longitudinal bunching also two cavities are used, the first one with a resonance frequency of 1.3 GHz and the second one with double the frequency.

SIMULATIONS

Alpha magnet

First the alpha magnet was modelled and simulated with CST (Computer simulation technology) to calculate the elements of the transport matrix. In Figure 2, the results are shown and compared with old simulations of Ref. [4]. The simulated magnet deflects the electrons by 270° in the horizontal plane. The discrepancy between the two results may explained by the fact that different algorithms are used. Furthermore the position of the beginning and the end of the alpha magnet can be different. The operating point will be chosen between 300 and 400 G to have little focusing in the x-direction and little dispersion. Furthermore the optical properties in both planes are quite similar.

Start-to-end

Simulation of the whole beamline is done successively with PARMELA (Phase and radial motion in electron linear accelerators) and CST. Both are particle in cell (PIC) codes. The resulting particle distribution of one program is used as a start distribution for the other one. In a first simulation, the source was simulated with CST [5] followed by a simulation with PARMELA of the beamline from the source to the first alpha magnet, which again is simulated with CST. The beamline downstream to the second alpha magnet, which is also simulated with CST, is simulated with PARMELA. The last part from the second alpha magnet to the injector

ISBN: 978-3-95450-190-8 doi:10.18429/JACoW-ERL2017-MOPSPP008

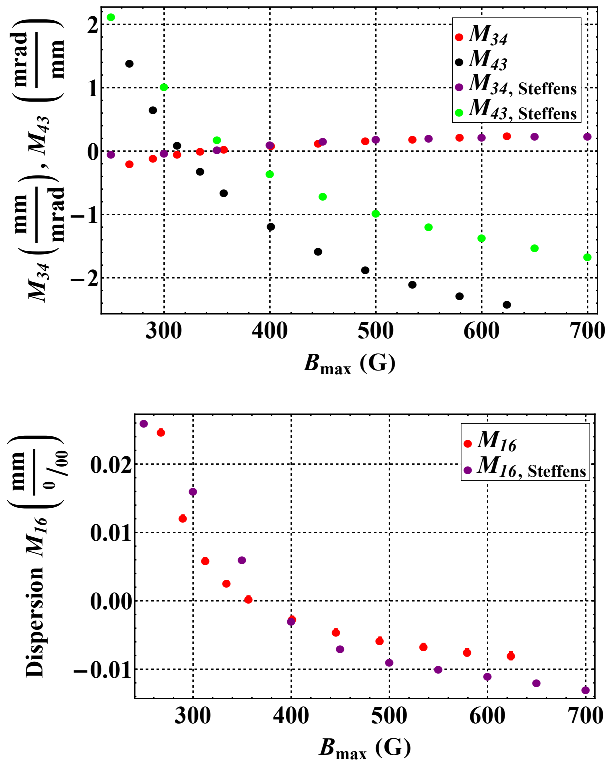

Figure 2: Elements of the transport matrix of the alpha magnet for different magnetic fields for an energy of 100 keV.

is simulated with PARMELA (see Fig. 3). Table 1 lists the beam parameters at the end of MELBA for 1.3 mA and 10 mA. For the smaller current, the beam has symmetric parameters in the x and the y plane, the emittances stay below our goal of 1.0 mm mrad, the loss of particles is 0 %.

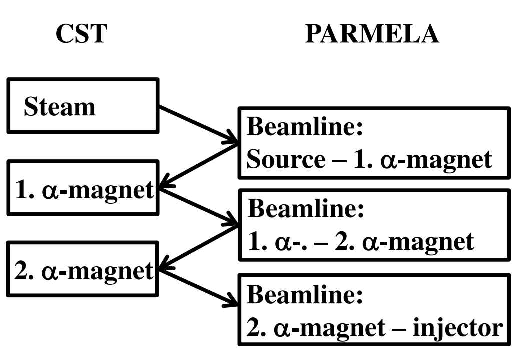

Figure 3: Parts of the beamline simulated with the two PIC codes CST and PARMELA.

In contrast, the parameters are higher and asymmetric, the goal of 1.0 mm mrad is exceeded, and there is a tremendous loss of 31.2 % with a beam current of 10 mA. The reason is the much higher space charge force, which can also be seen in Figure 7. Here in the xx' and yy' phase space of the

Table 1: Beam parameter at the end of MELBA, in front of the injector for two different currents. 1.3 mA and 10 mA correspond to 1 pC and 7.7 pC of bunch charge.

	1.3 mA	**10 mA**
x_{rms}	1.429 mm	1.713 mm
y_{rms}	1.442 mm	1.396 mm
x'_{rms}	5.887 mrad	6.190 mrad
y'_{rms}	5.854 mrad	4.804 mrad
$\epsilon_{x,\mathrm{rms,n}}$	0.576 mm mrad	1.165 mm mrad
$\epsilon_{y,\mathrm{rms,\,n}}$	0.484 mm mrad	1.111 mm mrad
$\Delta\phi_{\mathrm{rms}}$	2.044°	3.947°
$\Delta E_{\mathrm{kin,\,rms}}$	1.777 keV	2.084 keV
Loss of particle	0 %	31.2 %

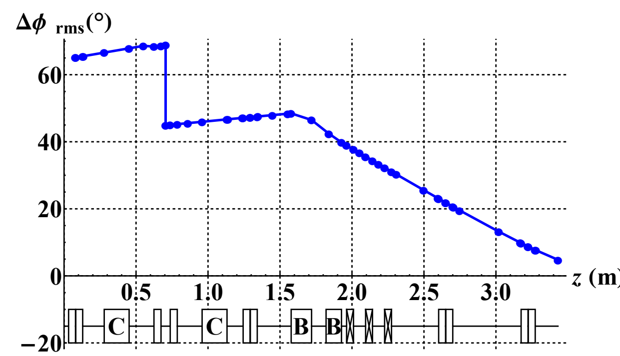

Figure 4: Longitudinal dimension along the beamline from the second alpha magnet to the injector for 10 mA.

10 mA beam, a strong filamentation is recognizable that is the result of the nonlinear space charge force.The explanation for the huge loss of particles is the natural elongation of the bunches due to the space charge. During the first 7.4 m of beamline from the source to the chopper system the longitudinal dimension ϕ_{rms} of the beam increases from 24° to 69°. The chopper system allows the passing of particles only with

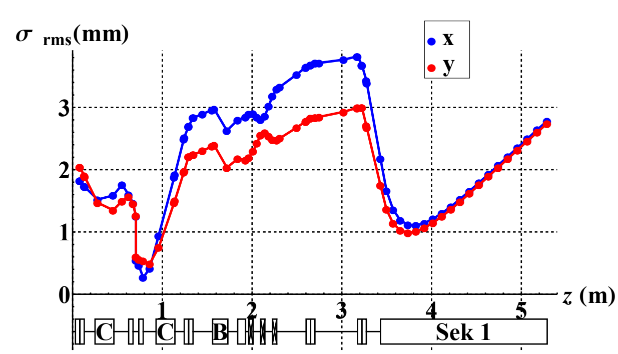

Figure 5: Transverse dimension along the beamline from the second alpha magnet to the end of the first section of the injector for 10 mA with 31.2 % of beam loss at the chopper collimator.

a maximum longitudinal phase distribution of ±80° around

ISBN: 978-3-95450-190-8 doi:10.18429/JACoW-ERL2017-MOPSPP008

the reference phase to match the beam with the longitudinal acceptance of the buncher system. Figure 4 depicts the rms value of the longitudinal dimension of the beam along the last part of the beamline behind the second alpha magnet. At the position of the collimator of the chopper system, a drop is observable. Nearly the complete loss of 31.2 % is dumped here as the beam has excessive longitudinal dimension. The decreasing longitudinal dimension afterwards is because of the longitudinal focusing of the buncher system. In addition the longitudinal focusing of the buncher causes increasing transverse space charge forces in front of and inside the injector. To avoid losses in this region, the transverse dimensions of the beam will be very large to minimize transverse space charge forces and then direct in front of the injector the beam will be strongly focused. With this the remaining 6.8 mA can pass the first section of the injector which depicts figure 5. In order to increase the possible beam current, decrease emittance growth and bunch elongation, the transverse beam size along the beamline should in general be as large and constant as possible. An approach to estimate the bunch

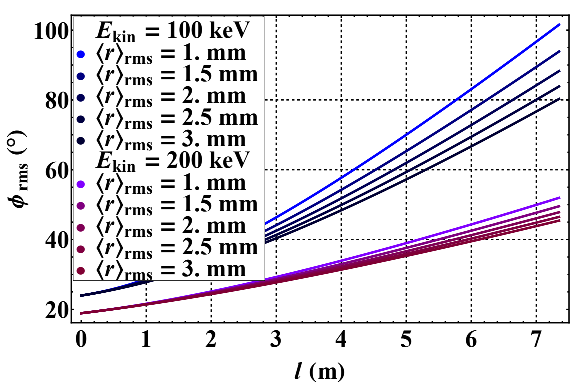

Figure 6: Bunch elongation along the beamline to the chopper collimator for 10 mA.

elongation can be the K-V equation [6]. In the transverse planes the dimensions were assumed to stay constant. Figure 6 shows the advantage of higher beam energy, larger average beam size, and shorter beamline.

Simulations of the whole beamline from the source to the injector show that 1.3 mA of beam current are possible to transport to the injector, whereas 10 mA are not because of the strong defocussing due to space charge.

STATUS MELBA

Currently, the source and the vertical part of MELBA consisting of a solenoid, a quadrupole triplet, a scanner, an alpha magnet and a part of the horizontal beamline consisting of two quadrupole triplets, a second scanner, and a differential pumping station is built up and baked out. The beamline ends with a small beam dump. The overall length is about 4 m. A sketch of the beamline can be seen in figure 8.

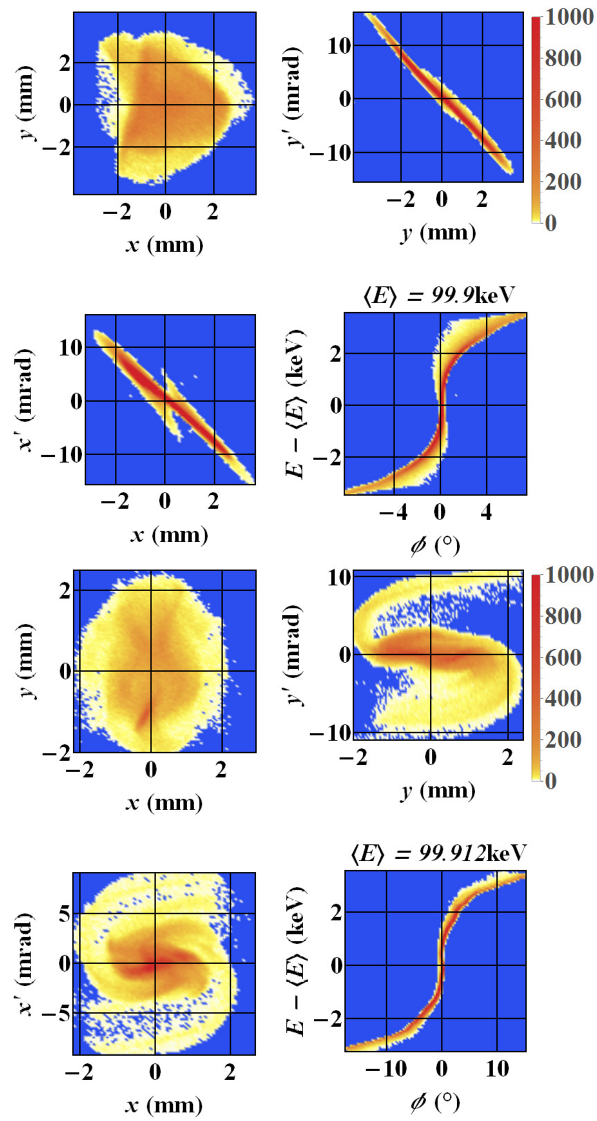

Figure 7: The upper four figures show the phase space for 1.3 mA and the lower ones the phase space for 10 mA. The unit of the legend is number of particle.

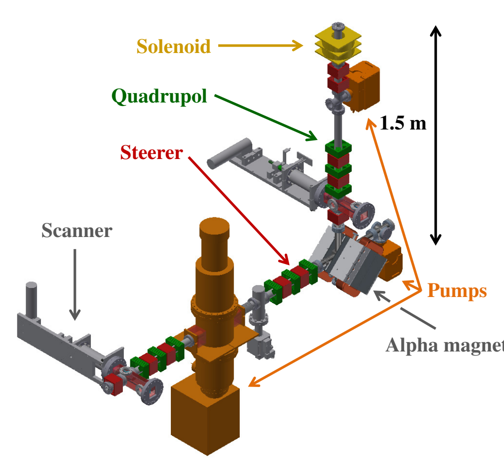

Figure 8: Current test setup of MELBA.

ISBN: 978-3-95450-190-8 doi:10.18429/JACoW-ERL2017-MOPSPP008

Diagnostics

At the moment, the only beam diagnostic devices are scanners. In comparison to the latest model of scanner at the institute, the needed bellows are guided to avoid twisting, and the target vacuum chamber is larger to allow the welding of a larger window flange to get a better sight inside. The available instruments are scintillator monitors made of YAG:Ce, wires (300 µm), and grids (25 µm). The scintillator monitors are couted with aluminium to ensure discharging of the electrons. A picture of them can be seen in Figure 9 (see also [7]). In addition to that, a moveable slit (71, 200 µm) was installed in the beamline 942 mm downstream of the source allowing to measure the emittance by shifting the beam over it by magnetic deflection. These techniques are similar to the ones in [8].

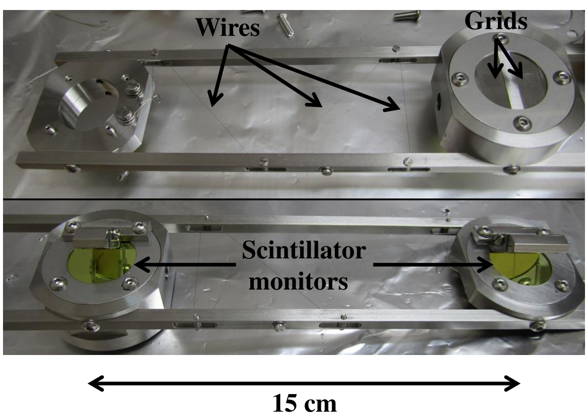

Figure 9: Mount with the diagnostic instruments. At the top the front of the instruments and at the bottom the back.

Vacuum System

As mentioned before, there is a differential pumping station [9] ensuring a good vacuum on the source side. Upstream to the source, there are two additional IGPs (ion getter pumps) and two pneumatic valves, which can separate the vacuum of the beamline. After baking out the whole beamline the pressure upstream of the differential pumping station reached 3×10^{-10} mbar and downstream 4×10^{-10} mbar. The pressure in vacuum chamber of the source stays on a lower level, namely 6×10^{-12} mbar. This is important to ensure a longer lifetime of the cathodes.

Quadrupoles

Since the Wien filters have an asymmetric aperture and one is very small, the use of quadrupoles was choosen. The beam will be focussed stronger in one plane in order to minimize space charge forces in the Wien filter. The yokes of the used quadrupoles are made of alternating aluminum and μ-metal plates. On the one hand this fabrication method allows a small remanence and on the other hand an increased length of homogeneous field compared to the fringe field.

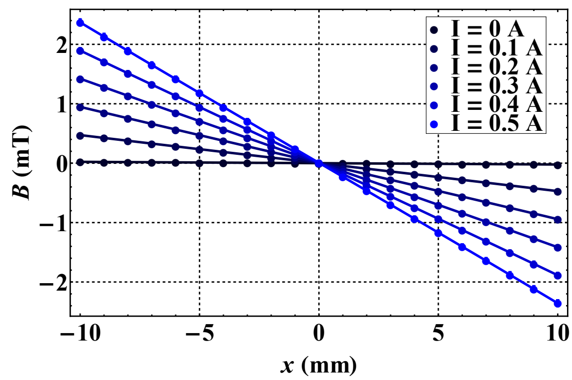

Figure 10: Measurement of the magnetic field along the transvers axis yields $\frac{dB}{dx \cdot I} = 0.4688(4)\,\mathrm{T\,m^{-1}\,A^{-1}}$.

Chopper System

An essential part of the chopper system are the cavities that deflects the beam circularly. The prototype [10] was improved by using copper instead of indium gaskets so the cavities are bakeable. Furthermore, the tuner flange now has the correct thickness for a better tuning of the cavity.

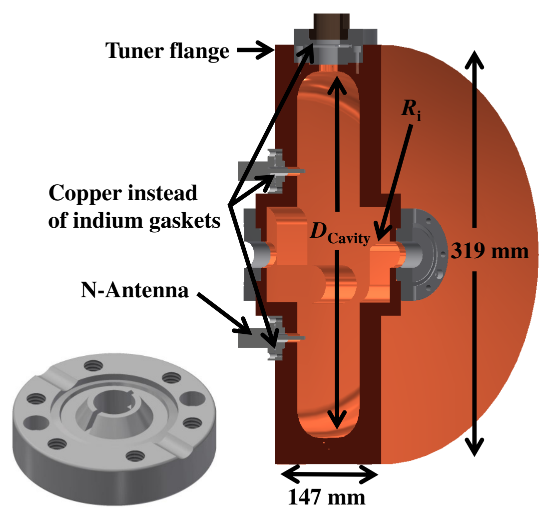

Figure 11: Half view of one chopper cavity.

Manufacturing is done in several steps, because only with the correct geometric form the resonance frequency and the field shape are the required ones, namely 1.3 GHz and a circular-deflecting field. With the chopper cavities the opportunity was taken to test flanges with nose cones shown in figure 11. They can help to avoid wake fields. Figure 12 shows electric field measurements (blue) and simulations with the current geometry (red) and the nominal field (black) before the last fabrication step of the cavities. In order to measure the field, a bead is pulled through the cavity, disturbing the field. This leads to an shift of the resonance frequency Δf which is proportional to E^2. Additionally the behaviour of the frequency while moving the tuner was measured. Figure 13 presents the measurement, that is in good agreement with the simulation result of $1.455 \times 10^5\,\mathrm{Hz\,mm^{-1}}$. More-

ISBN: 978-3-95450-190-8 doi:10.18429/JACoW-ERL2017-MOPSPP008

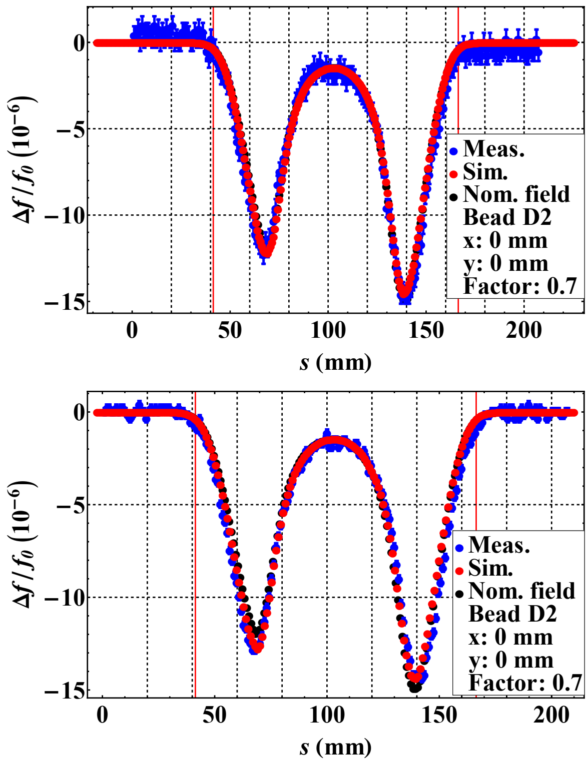

Figure 12: Measurements and simulations of the electric field on the reference axis in the chopper cavities.

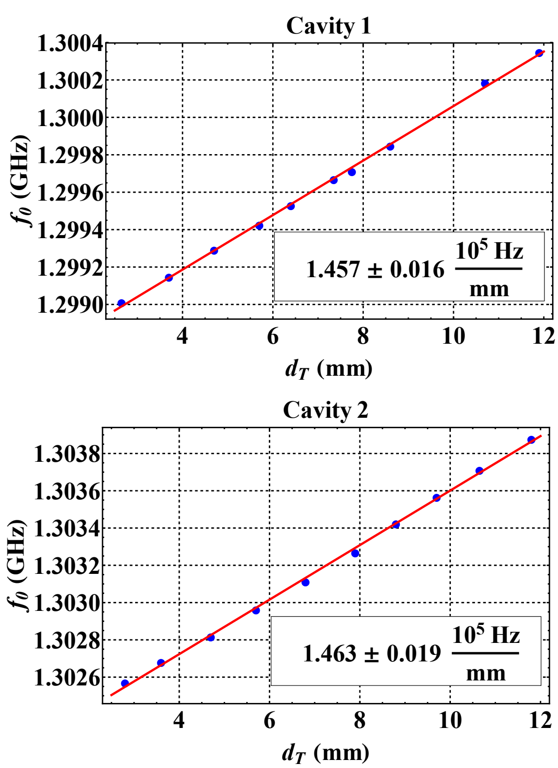

Figure 13: Tuner range measurement with line of best fit.

over the collimator system and the solenoids are fabricated and tested ([11], [12]).

CONCLUSION

In the first stage of MESA the current will be limited to about 1 mA since the modified ELBE (Elektronen Linearbeschleuniger für Strahlen hoher Brillanz und niedriger Emittanz) Cryomodules foreseen for the main accelerator cannot stand the HOM (higher order modes) power of currents significantly exceeding this value [13]. The analysis in the second chapter show that operating MELBA at the relatively low kinetic energy of 100 keV is compatible with this conditions. However, operating at currents of the order of 10 mA, planned in second stage of MESA, require either a source providing electrons with higher energy or a shorter low energy beamline. The latter will result in lower flexibilty concerning spin rotation. The source and first 4 m of beamline of MELBA have successfully been built up. The next steps will be the krypton gas processing of the source, assembling a LASER system, implementation of the control system and an interlock system. After first measurements, the beamline will be extended with the chopper and buncher system to prove their functionality.

REFERENCES

[1] PARMELA, Phase and radial motion in electron linear accelerators, 2005

[2] CST STUDIO SUITE 2016, Computer simulation technology

[3] K. Aulenbacher, *Erzeugung intensiver hochpolarisierter Elektronenstrahlen mit hoher Symmetrie unter Helizitaetswechsel*. Mainz, Germany, Shaker, 2007.

[4] K. Steffens, "Konzeption und Optimierung eines 100 keV Injektionssystems zur Erzeugung eines longitudinalen polarisierten Elektronenstrahls an MAMI", Ph.D. thesis, Phys. Dept., Institut für Kernphysik, Mainz, Germany, 1993.

[5] S. Friederich and K. Aulenbacher, "The Small Thermalized Electron source At Mainz STEAM", in *Proc. ERL'17*, Genf, Switzerland, June 2017, paper MOPSPP005.

[6] M. Reiser, *Theory and Design of Charged Particle Beams*. Weinheim, Germany, Wiley-VCH, 2008.

[7] I. Alexander, K. Aulenbacher, V. Bechthold, B. Ledroit, and C. Matejcek, "Diagnostic test-beam-line for the mesa injector", in *Proc. ERL'15*, Stony Brook, NY, USA, June 2015, paper THIALH2069, pp. 91-96

[8] E. D. Cantero, W. Andreazza, E. Bravin, A. Sosa, "The status of beam diagnostics for the HIE-ISOLDE linac at CERN", in *Proc. IBIC'14*, Monterey, CA, USA, September 2014, paper WEPF13, pp. 565-568

[9] A. Bünning, "Auslegung einer differentiellen Pumpstufe für das niederenergetische Strahlführungssystem am Mainz energy-recovering superconducting accelerator",

ISBN: 978-3-95450-190-8 doi:10.18429/JACoW-ERL2017-MOPSPP008

Diploma thesis, Phys. Dept., Institut für Kernphysik, Mainz, Germany, 2016.

[10] V. Bechthold, “Eine Deflektor-Kavität für den MESA-Beschleuniger”, Diploma thesis, Phys. Dept., Institut für Kernphysik, Mainz, Germany, 2013.

[11] C. Stoll, "‘Solenoid-Fokussierungsmagnete für den niederenergetischen Strahltransport an MESA"‘, Master thesis, Phys. Dept., Institut für Kernphysik, Mainz, Germany, 2016.

[12] B. Ledroit, “Aufbau und Test des MESA-Choppers”, Master thesis, Phys. Dept., Institut für Kernphysik, Mainz, Germany, 2016.

[13] F. Schlander, K. Aulenbacher, R. Heine, and D. Simon, “Investigation of cryomodules for the Mainz energy-recovering superconducting accelerator MESA”, in *Proc. IPAC’14*, Dresden, Germany, June 2014, paper WEPRI013, pp. 2505-2507.